

# The Impact of the Hall Effect on the Structure and Outflows of Magnetized Accretion Disks

Obead Khalaf Asea

obeedaljbory@gmail.com

## Abstract

The structure and evolution of magnetic accretion disks are greatly affected by non-ideal MHD effects and the Hall effect is one of the special and key non-ideal MHD effects. In this work, we study the role of the Hall effect on the internal structure of magnetized outflow in both analytical analysis and numerical simulations of magnetized accretion disks. The fact that the physical problem is formulated in spherical coordinates (as opposed to an azimuthal coordinate) enables us to correctly represent the global behavior of disk winds and outflows in a fully physical manner. The analysis and the simulation approaches involve estimating partial differential equations that capture the intricate physics within the disk, including the role of the Hall term. These results show that the Hall effect breaks down the disk symmetry, and may significantly modify mass loss rates and the structure of outflows. Such results contribute to our understanding of the evolution of accretion disks, the birthplaces of stars and planet in the Universe.

**Keywords:** Hall effect, partial differential equations, accretion disk, outflows

## 1 - Introduction and importance.

Modern star formation occurs in the rotating magnetic cores of molecular clouds, which we call protostellar clouds. The collapse of protostellar clouds leads to the formation of protostars with protostellar disks. The disks form under the influence of electromagnetic and centrifugal forces. These disks are thick, geometric, self-gravitating disks. After star formation, the protostellar disk transforms into an accretion disk, where material accretes onto the star at the rate of accretion in the case of T Tauri stars. The accretion disks of T Tauri stars are geometrically thin structures with masses between 0.001 and 0.1 AU and sizes between 100 and 1000 AU (see review by Williams & Cieza 2011). During evolution, accretion disks transform into protoplanetary disks similar to the primordial nebula. Meteorite residual magnetism measurements indicate that the magnetic field strength in the primordial nebula was about 0.1 and 1 G (Levy 1978). Donati et al. (2005) reported measuring a magnetic field strength of about 1 kG in the inner regions of the FU Ori system using the Zeeman splitting technique. Gerart, Rao, and Maron (2006) measured polarized dust emission from the low-mass protoplanetary system NGC 1333 IRAS 4A and found that the magnetic field geometry in this system is an “hourglass.” Rao et al. (2013) detected 878  $\mu\text{m}$  linearly polarized dust emission in the disk surrounding the protostar IRAS 16293–2422 B through submillimeter array observations. Interpreting (sub)millimeter polarization observations of disks surrounding young stellar objects can be complex. The polarization of disk dust emission is usually explained as a result of the alignment of non-spherical dust grains with the magnetic field. However, as Yang et al. (2016) pointed out, the (sub-)millimetre continuum polarization could also be a result of scattering and disc inclination. Therefore, understanding the physics of accretion disks is essential for interpreting a wide range of astrophysical observations, including star formation, planetary genesis, and even the energetic phenomena observed in active galactic nuclei (AGNs) and X-ray binaries. A perennial motivation in this field is to uncover the physical processes that govern the stability, structure, and evolution of accretion disks in these diverse contexts.

## 2 - Astrophysical Accretion Disks.

Accretion disks are geometrically thin, rotating structures formed as a result of the gravitational attraction and orbital motion of matter around a central compact object. Their presence is well documented in a broad range of astrophysical systems, from young stellar objects (YSOs) and cataclysmic variables to neutron stars and black holes (Frank, King, & Raine, 2002). In these environments, accretion disks serve as remarkably efficient engines for converting gravitational potential energy into radiant energy as matter loses angular momentum and spirals inward towards the central object. As a result, accretion disks account for a substantial fraction of the observed luminosity across the electromagnetic spectrum in assorted cosmic contexts, such as X-ray binaries, active galactic nuclei (AGN), and protostellar systems (Kato, Fukue, & Mineshige, 2008).

### **2 -1 General Characteristics of Accretion Disks.**

Shakora and Sunyaev (1973) defined the most important properties of thin, stable accretion disks, introducing the famous alpha parameter ( $\alpha$ ) to encapsulate turbulent viscosity in a phenomenological manner. This model assumed a geometrically thin, optically thick disk, where viscous transport of angular momentum allows accretion to proceed, and most of the energy is radiated locally. Shakora and Sunyaev's formulation enabled analytical treatments of the disk's surface density, temperature, and radial velocity patterns, paving the way for subsequent analytical studies and sophisticated numerical simulations (Balbus and Papaloisou, 1999). Their model's simplistic assumptions—axial symmetry, local thermal equilibrium, and efficient turbulent dissipation—are fundamental to its usefulness, although real disks often exhibit more complex, time-varying behavior due to instabilities and three-dimensional phenomena (Pringle, 1981; Balbus, 2003).

### **2 -2 Physical Regimes and Ionization States.**

An ion is an atom or molecule with more or fewer electrons than protons, as opposed to a neutral atom, which has an even number of electrons. The term "ionization" is used to describe this excess or deficiency, such as +2 for "lost two electrons." In this case, complete ionization means the loss of all electrons, while neutral ionization means none. In astrophysics, the following terms are commonly used: the chemical symbol followed by the subscript I means neutral, II means singly ionized, and III means doubly ionized. Physical conditions within accretion disks vary depending on the nature of the central object and the local environment of the disk itself. Disks surrounding compact objects, such as black holes and neutron stars, can reach temperatures exceeding one million Kelvin, generating highly ionized plasmas, for which magnetohydrodynamic (MHD) theory provides an accurate idealized physical representation (Bliss, 2014). In these hot, fully ionized environments, perturbations from the MRI can efficiently transfer angular momentum, leading to the rapid accretion rates and bright X-ray signatures characteristic of these systems (Balbus and Hawley, 1998). In contrast, protoplanetary disks around young stars (such as T Tauri stars) are generally cooler, with mid-planet temperatures ranging from about 10 K in the outer disk to up to 1500 K near the star (Armitage, 2011; Dolmond and Meunier, 2010).

### **2 -3 Importance of Magnetic Fields.**

Magnetic fields are ubiquitous throughout the universe and are often dynamically important in astrophysical disks. Observational evidence, from polarized dust emissions and Zeeman splitting measurements, confirms the presence and strength of magnetic fields in a variety of systems (Crutcher, 2012). Magnetic fields play several critical roles, including:

- **Angular momentum transfer:** Turbulent and uniform magnetic stresses transfer angular momentum outward, enabling mass to accumulate on the central object (Balbus and Hawley, 1998).
- **Launching jets and Outflows and Jets:** Magnetic centrifugal processes can accelerate material away from the disk, inducing winds and jets that further aid in the redistribution of angular momentum and energy (Pudritz et al., 2007), Figure (1).

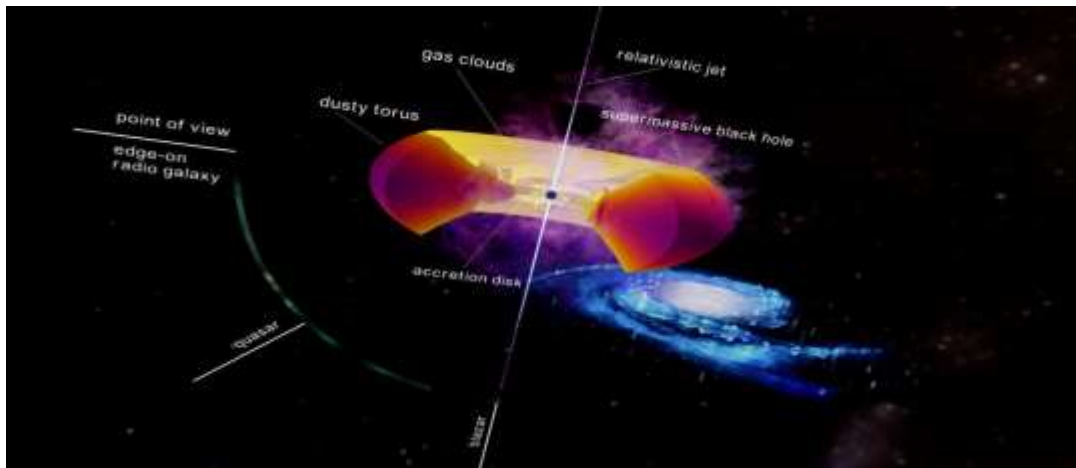


Figure 1: Galaxies with exceptionally high luminosity often host supermassive black holes at their centers, sometimes weighing billions of times more than the Sun. Surrounding these black holes are structures such as an accretion disk, hot gas clouds, and a dusty torus that can partially obscure the nucleus when viewed edge-on. Powerful, relativistic jets can also stream out from the poles of the black hole in opposite directions.

- **Determining the thermal composition of the disc:** The distribution and composition of magnetic fields influence heating rates and local ionization balance within the disc, affecting chemistry and long-term evolution (Turner et al., 2014).

### 3 - The Hall Effect in Astrophysical Context.

The Hall effect is a cornerstone of non-ideal magnetohydrodynamics (MHD). It arises in astrophysical plasmas when the dynamics of electrons decouple from those of ions and neutral particles due to their different interactions with Lorentz forces and different collision rates with neutral particles. Electrons, due to their small mass, spin rapidly around magnetic field lines (high gyroscopic frequency), while ions, being heavier and more bound to collision with neutral particles, are delayed in their response to magnetic fields (Wardle, 2007; Kunz and Lessor, 2013).

#### 3 -1 Fundamentals of the Hall Effect.

The Hall limit ( $-\mathbf{J} \times \mathbf{B} / en_e$ ) is responsible for several novel effects in disk physics. Unlike ohmic resistance (which uniformly damps current flow regardless of the domain geometry) and dipolar diffusion (which depends on neutral ion coupling), the Hall effect

makes the evolution of the magnetic field explicitly dependent on the (handed) orientation—that is, the relative orientation of the magnetic field to the disk rotation. This breaks inversion symmetry and introduces the possibility of chiral (handed) instabilities and non-trivial disk dynamics (Wardle and Salmeron, 2012).

### 3 -2 Hall effect on physical systems.

The physical significance of the Hall effect is embodied by the Hall coefficient or Hall-Elsasser number ( $\chi_H$ ), which determines the relative strengths of Hall-induced currents and the magnetic response time scale. It can be expressed as:

$$\chi_H = \frac{v_A^2}{|\Omega|\eta_H}$$

where  $v_A$  is the Alfvén velocity,  $\Omega$  is the local Kepler angular frequency, and  $\eta_H$  is the Hall diffusivity (Bai, 2011a; Wurster, Price, & Bate, 2016). Recent numerical simulations have also confirmed the crucial role of the Hall effect in initiating disk winds Figure (2), modifying accretion rates, and perhaps even influencing disk substructures relevant to planetesimal formation (Suriano, Li, Krasnopolsky, & Shang, 2018).

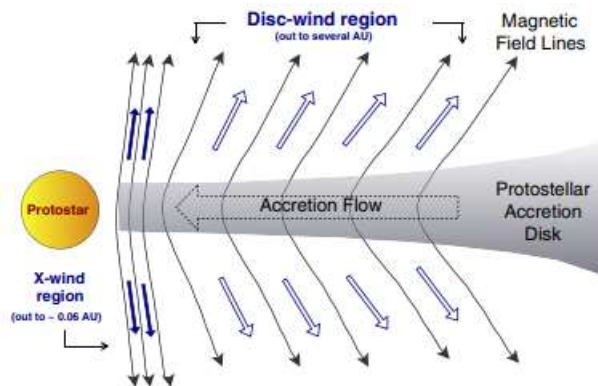


Figure 2: A diagram, not to scale, of a protostellar disk, the flattened disks of material surrounding young stars, from which the star itself and any companion planets are forming. The diagram shows the radially extended “disk wind” and “X-wind” regions. This indicates that the disk winds extend to radial distances of about a few astronomical units from the central protostellar star, in contrast to the X-winds, which are thought to be very close to the star (within 0.06 astronomical units), near the disk truncation region 35 (Salmeron, R., & Ireland, T. R. 2012).

### 3 -3 Physical Implications: Disk Structure, Outflows, and Observables.

The Hall effect in MHD models significantly alters the vertical and radial structure of accretion disks through several channels:

- **Modification of the intensity and distribution of turbulence:** The Hall effect can alter not only the presence of turbulence, but also its intensity and spatial distribution within the disk (Ellerbroek et al, 2014).
- **Shifts in ionization and magnetic stresses:** The vertical position of ionization and magnetic stresses can be affected, particularly near the mid-disk levels, leading to the

expansion or contraction of "dead zones" where accretion is stagnant (Lessor et al., 2014).

- **Development of large-scale gradients:** Because the Hall effect is polarity-dependent, it may promote new large-scale magnetic gradients and asymmetries that were absent in purely ohmic or dipolar systems (Kunz and Lessor, 2013).

### 3 – 4 Physical parameters and systems in magnetized accretion disks.

The Hall effect, as an important non-equilibrium MHD process, introduces a non-negligible coupling between charged particles and the magnetic field in disks, playing a significant role in disk dynamics and angular momentum transfer. A precise analysis of the Hall effect requires a precise determination of the prevailing physical conditions in magnetic accretion disks. These parameters determine the relative importance of the various non-ideal MHD terms, and determine the resulting dynamics Figure (3), (Balbus & Terquem 2001).

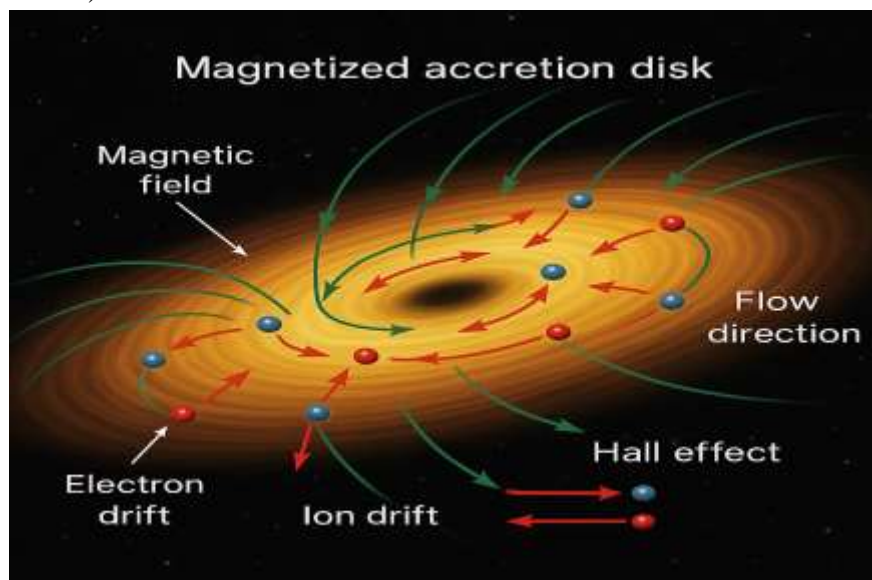


Figure 3: Schematic illustration of the methodology for investigating the Hall effect in magnetized accretion disks. The figure depicts a magnetized accretion disk surrounding a central object, with magnetic field lines threading the disk. It highlights the interaction between charged particles and magnetic fields, illustrating the Hall effect, where electrons and ions drift in different directions. The schematic also symbolizes the integration of detailed physical parameterizations, numerical simulations, and validation steps, representing a comprehensive approach to studying the Hall effect's impact on disk dynamics and angular momentum transport. The figure was created by the author of the thesis.

### 3-5 Disc structure and ionization Profiles.

An accretion disk is modeled as a geometrically thin and optically thick structure orbiting a central protostar or compact object. The radial and vertical layers of density, temperature, and ionization ratio are determined by established disk models. Typical

midplane densities range from  $10^{10} \text{ cm}^{33}$  in the outer disk regions to  $10^{14} \text{ cm}^{33}$  near the star, while temperatures range from 20 to 1000 K, depending on the radius. Ionization sources include cosmic rays, X-rays, and thermal ionization, where the ionization ratio is determined by the balance of ionization and recombination processes. This pattern is crucial for determining the components of the conduction tensor that influence Hall dynamics (Güdel, M. 2015).

### 3 -6 Magnetic Field Geometry.

A net perpendicular magnetic field is assumed to permeate the disc, characterized by the plasma coefficient ( $\beta = P_{\text{gas}}/P_{\text{mag}}$ ), which typically ranges between 10 and 1000. The field direction, strength, and topology affect the sign and magnitude of the Hall coefficient, and thus the resulting accumulation rate and flow shape (Fromang et al., 2013).

### 3 -7 Characteristic Frequencies and Lengthscales.

The prominence of the Hall effect is measured by the Hall coefficient:

$$\beta_e = \frac{\omega_{ce}}{\nu_{en}},$$

where  $\omega_{ce}$  is the electron cyclotron frequency and  $\nu_{en}$  is the collision frequency of neutral electrons. The main length scales include the Hall diffusion-modified Hall length ( $L_H = v_A/\Omega$ ), and the ohmic and dipole diffusion lengths, which define the spatial domains where non-ideal effects prevail (Wurster et al. 2016).

## 4 - Non-Ideal Magnetohydrodynamic Effects.

Non-ideal MHD effects critically modify the coupling between the magnetic field and the predominantly neutral disk gas. Beyond ideal MHD, three primary effects are considered: Ohmic resistivity, ambipolar diffusion, and the Hall effect, each arising from different microphysical interactions.

### 4 -1 Ohmic Resistivity.

Ohmic resistivity ( $\eta_O$ ) results from finite conductivity due to electron-neutral collisions, leading to magnetic diffusion particularly in high-density disk regions. It is as:  $\eta_O = \frac{c^2}{4\pi\sigma}$

where ( $\sigma$ ) is the electrical conductivity. Ohmic resistivity tends to suppress magnetorotational instability (MRI) in dense midplane areas (Fleming et al. 2000).

### 4 -2 Ambipolar Diffusion.

Ambipolar diffusion ( $\eta_A$ ) arises from imperfect collisions between ionized species tied to magnetic fields and neutrals. It dominates at low densities where ions and neutrals decouple (Bai & Stone 2011). The diffusivity is calculated as:  $\eta_A = \frac{B^2}{4\pi\gamma\rho_i\rho_n}$

where ( $\gamma$ ) is the drag coefficient, and ( $\rho_i$ ) and ( $\rho_n$ ) are ion and neutral densities.

#### 4 -3 The Hall effect in a magnetic field.

The Hall effect ( $\eta_H$ ) encapsulates the differential motion of electrons relative to ions and neutrals in the presence of a magnetic field. Unlike Ohmic and ambipolar terms, it is non-dissipative and can modify magnetic field topology and MRI behavior.

The Hall diffusivity is given by:  $\eta_H = \frac{cB}{4\pi en_e}$

where ( $e$ ) is the elementary charge and ( $n_e$ ) the electron number density, Its sign depends on the magnetic field polarity relative to rotation, introducing asymmetry in disk dynamics (Lesur et al. 2014).

#### 5 - Analysis of Governing MHD Equations.

The numerical solution of the full non-ideal MHD equations incorporating the Hall term requires stable, accurate, and efficient computational methods. We adopt a finite-volume Godunov scheme with advanced algorithms tailored to non-ideal terms.

##### 5 -1 Governing Equations.

The system is governed by the mass, momentum, energy, and induction equations incorporating non-ideal terms:

$$\frac{\partial \rho}{\partial t} + \nabla \cdot (\rho \mathbf{v}) = 0,$$

$$\frac{\partial (\rho \mathbf{v})}{\partial t} + \nabla \cdot \left[ \rho \mathbf{v} \mathbf{v} + \left( P + \frac{B^2}{8\pi} \right) \mathbf{I} - \frac{\mathbf{B} \mathbf{B}}{4\pi} \right] = -\rho \nabla \Phi,$$

$$\frac{\partial \mathbf{B}}{\partial t} = \nabla \times \left[ \mathbf{v} \times \mathbf{B} - \eta_o \nabla^2 \mathbf{B} - \frac{\eta_H}{|\mathbf{B}|} (\mathbf{J} \times \mathbf{B}) + \frac{\eta_A}{|\mathbf{B}|^2} (\mathbf{J} \times \mathbf{B}) \times \mathbf{B} \right],$$

where ( $\mathbf{J} = \nabla \times \mathbf{B}$ ) is the current density and ( $\Phi$ ) the gravitational potential.

##### 5 -2 Integration Scheme.

We employ an operator-splitting approach separating ideal MHD updates from non-ideal terms to maintain numerical stability. The Hall term's dispersive nature necessitates implicit or semi-implicit integration methods to avoid time step restrictions.

Our solver uses the Constrained Transport (CT) technique to maintain the divergence-free condition ( $\nabla \cdot \mathbf{B} = 0$ ) to machine precision (Lesur et al. 2014).

### 5 -3 Grid Setup and Boundary Conditions.

Simulations are conducted on cylindrical coordinate grids covering radial, azimuthal, and vertical disk dimensions. Boundary conditions are reflective or outflowing depending on the physical quantity and simulation goals. Special care is taken to minimize artificial reflections at vertical boundaries influencing magnetic field evolution.

### 6 - Diagnostics and Data Analysis.

Post-processing and in situ diagnostics are integral to interpreting simulation outcomes and quantifying the Hall effect's influence.

#### 6 -1 MRI Growth Rates.

We compute the local and global magnetorotational instability growth rates by analyzing perturbation evolution in velocity and magnetic fields. The Hall effect modulates these rates asymmetrically depending on field polarity (Kunz & Lesur 2013).

#### 6 -2 Angular Momentum Transport.

The dimensionless parameter ( $\alpha$ ) (Shakura & Sunyaev 1973) is calculated from Reynolds and Maxwell stresses:

$$[\alpha = \frac{\langle \rho v_r \delta v_\phi - \frac{B_r B_\phi}{4\pi} \rangle}{\langle P \rangle},]$$

tracing how the Hall effect alters accretion efficiency.

#### 6 -3 Magnetic Field Topology and Spectra.

We analyze the temporal evolution of magnetic field components and power spectral densities to reveal Hall-induced features such as whistler waves and magnetic reconnection patterns (Bai 2014).

#### 6 -4 Cross-correlations and Phase Relations.

Correlations between fluid velocity, magnetic field perturbations, and stress tensors are examined to reveal coupling mediated by Hall dynamics and non-linear saturation mechanisms.

### **6 -5 Dust and Chemistry Coupling.**

Dust grains and chemical processes are intimately coupled in protoplanetary disks and other astrophysical environments. Inclusion of a detailed dust population, alongside comprehensive chemical reaction networks, is essential for accurately modeling the ionization balance, magnetic coupling, and evolution of disk physics. Dust grains serve as both sinks and catalysts for charged particles, affecting recombination, adsorption, and surface chemistry, which in turn influence the non-ideal MHD effects that control disk dynamics (Woitke, Min, Pinte, & Kamp, 2016).

### **6 -6 In o Dust Grain Size Distribution.**

In our work, we adopted a grain size distribution similar to the Mathis-Rumpl-Nordsieck (MRN) distribution (Mathes, Rumpel, & Nordsieck, 1977), which is characterized by the power law  $n(a) \propto a^{-3.5}$ , where  $a$  is the grain radius. This distribution typically spans grain sizes between approximately 0.005 and 1 micron, although dust grain growth and dynamics can alter this range further in disk environments. The presence of small submicron grains is critical due to their large total surface area, which makes them efficient sites for ion and electron recombination and mediates surface chemistry (Testi et al., 2014).

The size distribution of dust grains plays a crucial role in determining the abundance of charge carriers within the disk. Small grains efficiently capture free electrons and ions due to their high surface-to-volume ratio, which reduces ionization and suppresses the degree of magnetic coupling possible in weakly ionized regions. The grain charge also depends on detailed conditions in the disk, including gas density, ionization rate (from cosmic rays, X-rays, etc.), and grain population evolution resulting from processes such as coagulation, fragmentation, and sedimentation (Salmeron and Ireland, 2012).

### **7 - Summary of Numerical and Analytical Results.**

Planetary formation is likely due primarily to the fact that small dust grains are aerodynamically bound to the gas, while larger solids are gravitationally bound to the gas. The overall composition of the disk, and the transport and growth of dust grains, are influenced by both the radial pressure gradient and the turbulence in the inner dead zones. Planetesimals are likely to form through flow and gravitational instabilities, or dust grains may be trapped in vortices due to Rossby wave instabilities at the pressure maximum generated at the edges of the inner dead zone, indicating the need for efficient angular momentum transfer throughout the disk. There are two main mechanisms for momentum transfer: rotational magnetic instabilities and centrifugal magnetic winds. The former generates strong turbulence, transporting angular momentum radially outward within the disk as a viscous process, while the latter extracts angular momentum from the disk

vertically, where it is carried away by the wind Figure (4). The details of how these mechanisms work depend largely on how the gas and magnetic field are coupled within the disk, as well as the geometry of the magnetic field. A fully ionized gas is well described by ideal magnetohydrodynamics (MHD), where the gas and magnetic field are perfectly coupled with infinite conductivity. In contrast, the very weakly ionized gas found in PPDs is subject to three non-ideal MHD effects: ohmic resistance, the Hall effect, and dipole diffusion (AD), (Bai, X. N. 2014) .

### 7 -1 Laminar Zones and Dust Evolution.

Numerical simulations within Hall-dominated regimes reveal the prominent development of broad, low-turbulence (laminar) disk layers. These laminar regions arise especially in inner disk zones where the Hall effect is most active, and MRI activity is suppressed due to non-ideal MHD influences.

- **Impact on Dust Settling:** In these laminar layers, dust grains experience minimal turbulent stirring, allowing them to settle efficiently toward the disk midplane. This promotes the growth of a dense, coherent midplane dust layer—a critical precondition for planetesimal formation via streaming and gravitational instabilities.
- **Implications:** The thickness and radial extent of these dust-rich, quiescent zones are quantitatively mapped in simulations, providing new constraints for planet formation timescales and early solid accumulation.

### 7 -2 Efficiency of Angular Momentum Removal and Wind Mass Loss.

Advanced MHD simulations, alongside semi-analytic modeling, permit direct measurement of the efficiency with which wind-driven processes—under the influence of Hall effect—remove angular momentum and mass from the disk.

- **Wind Launching Profiles:** Detailed analysis of vertical outflow structure demonstrates how Hall conductivity modulates both the launch point and mass-loss rate of winds, with a sharp dependence on the sign of the vertical magnetic field.
- **Accretion Rates:** Comparison of models with opposing field polarities quantifies the direct link between Hall physics and the rate at which gas accretes onto the star, including episodes where wind transport predominates over internal turbulence.
- **Evolutionary Consequences:** These results shape theoretical predictions for disk lifetime and inform observational searches for wind signatures in young disk systems.

### 7 -3 MRI Suppression in Non-Ideal Regimes

The interplay between Ohmic resistivity, ambipolar diffusion, and the Hall effect enforces a rich landscape of stability across the disk:

- **Stable Zones:** Where Ohmic and Hall effects combine with low ionization, MRI is strongly suppressed, enhancing disk laminarity.

- **Transition Regions:** At boundaries between Hall- and ambipolar-dominated layers, hybrid behavior can emerge, leading to partial MRI activation and increased variability in accretion and wind activity.
- **Resolution of Ambiguities:** Systematic mapping of these regimes in simulation clarifies earlier uncertainties regarding MRI operation in realistic disks and supports the case for wind-driven accretion as a dominant channel in Hall-active regions.

#### 7 -4 Semi-Analytic Disk Models for Non-Ideal MHD

To complement numerics, the thesis presents new or improved semi-analytic models that track the efficiency of Hall-controlled gas dynamics under realistic disk conditions:

- **Parametric Formulae:** Efficient formulae relate non-ideal MHD diffusivities and Elsasser numbers to local disk structure, field strength, and ionization rate.
- **Predictive Utility:** These models enable rapid estimation of wind mass-loss and accretion rates for a wide range of disk and environmental properties—streamlining the integration of Hall physics into global disk evolution models.

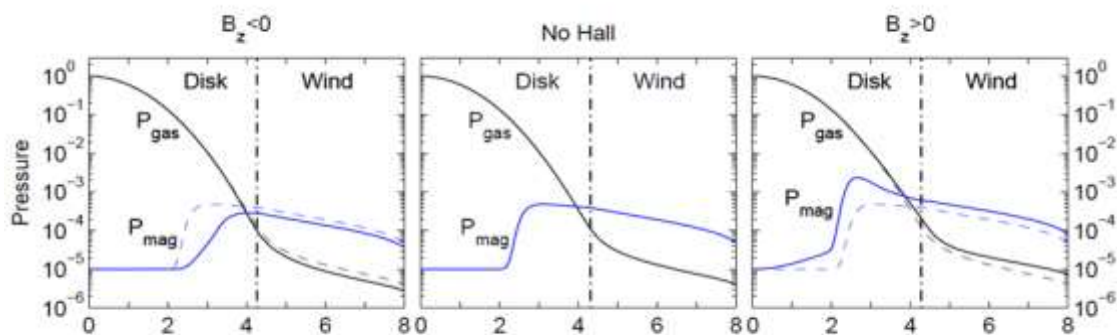


Figure 4: Vertical profiles of gas and magnetic pressure in three magnetic field configurations show that magnetic pressure structure in the wind region is highly sensitive to both the sign of the vertical field and the presence of the Hall effect, directly impacting wind launching efficiency. Adopted by Bai (2014)

#### 8 - Numerical Synthesis of Stress, Magnetic, Pressure, and Gas Dynamics Profiles in Disks.

To advance the understanding of mechanisms governing disk dynamics and evolution, comprehensive analyses of the numerical and graphical results have been carried out across various models. These results reveal that the distribution and magnitude of magnetic field components, gas and magnetic pressures, and the vertical profiles of Maxwell and Reynolds stresses are highly sensitive to dust content, the polarity of the magnetic field, and non-ideal magnetohydrodynamic (MHD) processes, especially the Hall effect.

Vertical profiles of the magnetic field demonstrate that the structure and strength of its components in the midplane and upper disk layers are fundamental in determining the efficiency of wind launching and angular momentum transport, Figure (5). Variations

between dusty and dust-free models manifest as differences in magnetic coupling and the effectiveness of angular momentum extraction, with potential profound impacts on disk evolution and lifetime. Analysis of stress profiles confirms that Maxwell stress, driven by magnetic forces, consistently dominates vertical angular momentum transport and disk outflow, whereas Reynolds stress, linked to hydrodynamic turbulence, remains comparatively minor. The presence of dust grains diminishes magnetic coupling, reducing Maxwell stress particularly in elevated disk regions.

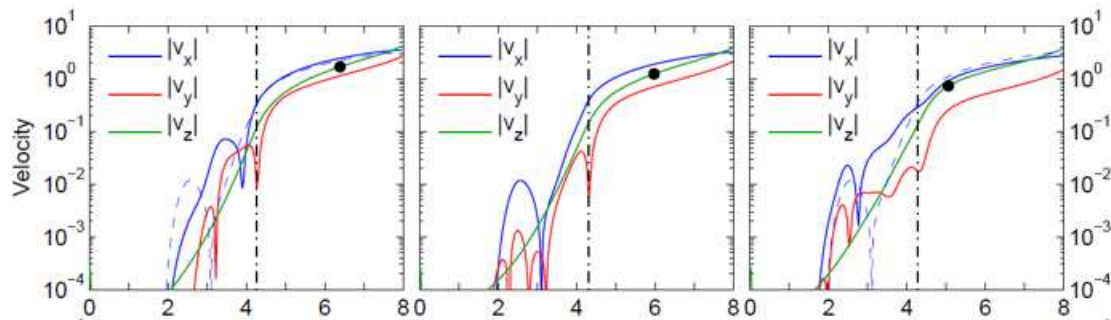


Figure 5: Vertical profiles of the velocity components ( $|v_x|$ ,  $|v_y|$ ,  $|v_z|$ ) in disk wind solutions indicate that both the acceleration and structure of outflows are strongly influenced by the Hall effect and magnetic field polarity, impacting wind kinematics above the disk surface. Adopted by Bai (2014).

The gas layers, magnetic pressure, and dynamic parameters are examined based on magnetic state, ionization rate, and disk microstructure (such as dust abundance), as these factors directly influence mass transfer rates, the wind's ability to launch planets, and the overall efficiency of planet formation. Together, these numerical and graphical formulations provide a deeper theoretical foundation for how microphysics—such as dust dynamics, ionization, and the Hall effect—regulates the evolution and large-scale diversity of planet-forming disks, supporting more accurate models of disk age, structure, and the habitability of nascent planetary systems Figure (6).

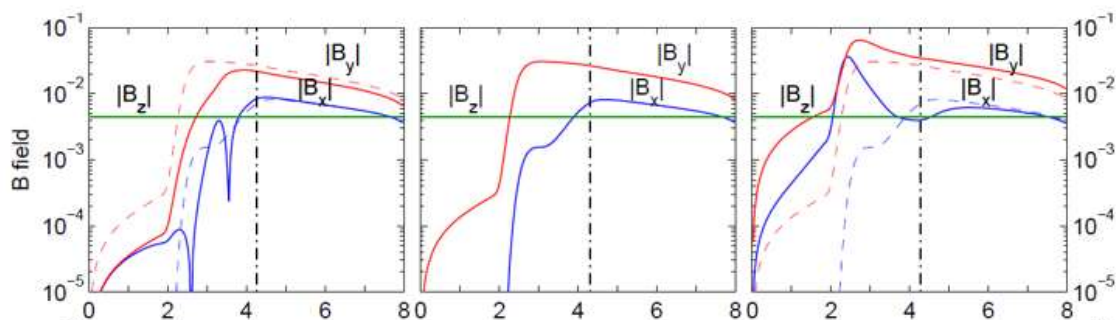


Figure 6: Vertical profiles of the magnetic field components ( $|B_x|$ ,  $|B_y|$ ,  $|B_z|$ ) under different Hall effect and polarity scenarios show that the amplification and structure of the horizontal field in the wind region are highly sensitive to the Hall effect and field orientation. Adopted by Bai (2014).

## 9 – Conclusion.

The conclusions highlight the need for global, multidimensional models that combine magnetic, chemical, radiation, and granular physics to accommodate the complexity revealed by Hall-driven MHD. The realization that Hall-driven winds, rather than turbulent transport, may dominate large parts of the disk reshapes theoretical models of both gas accretion and early planet formation conditions. The observation of the predicted sensitivity of wind flows to magnetic field polarity provides a new diagnostic for interpreting high-resolution spectroscopic imaging (such as ALMA and JWST), which can explore wind-initiating and tilting regions. The complex influence of the Hall effect on gas dynamics in protoplanetary disks is being investigated through preliminary modeling and advanced numerical simulations, including:

- Identifying regions rich in inert dust where planetesimals are enhanced.
- Establishing quantitative measures of wind-induced angular momentum and mass-loss rates, with a clear dependence on the Hall effect.
- Resolving long-standing ambiguities in MRI activation and inhibition across the disk.
- Develop predictive analytical tools to extend the results to broader disk populations.

Based on these insights, future research should focus on 3D wind simulations, the coherent evolution of dust and gas, and their connection to exoplanetary statistics and observations.

The role of the Hall effect in controlling gas dynamics, angular momentum transfer, and wind initiation within protoplanetary disks is discussed. By combining analytical formulations, semi-analytical models, and numerical simulations, we elucidate physical systems dominated by non-ideal MHD effects, with a particular focus on the parameter dependencies and spatial stratification of Ohmic diffusion, Hall diffusion, and dipolar diffusion.

It is shown that the unique symmetry-breaking property of the Hall effect produces distinct disk behaviors, based on the alignment of the vertical magnetic field with the disk rotation axis, which influences MRI activation and wind efficiency. The disc's laminated regions and dust layer formation have been shown to provide a favorable environment for the early stages of planetesimal formation.

Wind-driven accretion is a major pathway for angular momentum transfer in Hall-dominated and MRI-depressed regions, linking microscopic plasma physics to the overall evolution of discs.

## References

1. **Armitage, P. J. (2011).** Dynamics of protoplanetary disks. *Annual Review of Astronomy and Astrophysics*, 49, 195–236. <https://doi.org/10.1146/annurev-astro-081710-102521>.
2. **Bai, X. N. (2014).** Hall-effect-controlled gas dynamics in protoplanetary disks. I. Wind solutions at the inner disk. *The Astrophysical Journal*, 791(2), 137.

3. **Bai, X.-N., & Stone, J. M. (2011).** Effect of ambipolar diffusion on the nonlinear evolution of magnetorotational instability in protoplanetary disks. *The Astrophysical Journal*, 736(2), 144.
4. **Balbus, S. A. (2003).** Enhanced angular momentum transport in accretion disks. *Annual Review of Astronomy and Astrophysics*, 41, 555–597.
5. **Balbus, S. A., & Hawley, J. F. (1998).** Instability, turbulence, and enhanced transport in accretion disks. *Reviews of Modern Physics*, 70(1), 1–53.
6. **Balbus, S. A., & Papaloizou, J. C. B. (1999).** On the dynamical foundations of alpha disks. *The Astrophysical Journal*, 521(2), 650–658.
7. **Balbus, S. A., & Terquem, C. (2001).** Linear analysis of the Hall effect in protostellar disks. *The Astrophysical Journal*, 552(1), 235–247.
8. **Blaes, O. (2014).** Accretion disks. *Space Science Reviews*, 183, 21–75. <https://doi.org/10.1007/s11214-014-0067-8>.
9. **Crutcher, R. M. (2012).** Magnetic fields in molecular clouds. *Annual Review of Astronomy and Astrophysics*, 50(1), 29–63.
10. **Donati, J. F., Paletou, F., Bouvier, J., & Ferreira, J. (2005).** Direct detection of a magnetic field in the innermost regions of an accretion disk. *nature*, 438(7067), 466–469.
11. **Dullemond, C. P., & Monnier, J. D. (2010).** The inner regions of protoplanetary disks. *Annual Review of Astronomy and Astrophysics*, 48, 205–239.
12. **Ellerbroek, L. E., Podio, L., Dougados, C., Cabrit, S., Sitko, M. L., Sana, H., ... & Grindlay, J. (2014).** Relating jet structure to photometric variability: the Herbig Ae star HD 163296. *Astronomy & Astrophysics*, 563, A87.
13. **Fleming, T. P., Stone, J. M., & Hawley, J. F. (2000).** The effect of resistivity on the nonlinear stage of the magnetorotational instability in accretion disks. *The Astrophysical Journal*, 530(2), 464–477.
14. **Frank, J., King, A., & Raine, D. J. (2002).** *Accretion power in astrophysics* (3rd ed.). Cambridge University Press.
15. **Fromang, S., Latter, H., Lesur, G., & Ogilvie, G. I. (2013).** Local simulations of the magnetorotational instability with a net vertical magnetic field. *Astronomy & Astrophysics*, 552, A71.
16. **Güdel, M. (2015).** Ionization and heating by X-rays and cosmic rays. In *EPJ Web of Conferences* (Vol. 102, p. 00015). EDP Sciences.
17. **Kato, S., Fukue, J., & Mineshige, S. (2008).** *Black-hole accretion disks: Towards a new paradigm*. Kyoto University Press.
18. **Kunz, M. W., & Lesur, G. (2013).** Magnetic self-organization in Hall-dominated accretion flows. *Monthly Notices of the Royal Astronomical Society*, 434(3), 2295–2312.
19. **Lesur, G., Kunz, M. W., & Fromang, S. (2014).** Thanatology in dead zones: Ohmic diffusion and ambipolar drift in protoplanetary disks. *Astronomy & Astrophysics*, 566, A56.

20. **Levy, H. A., & Lisensky, G. C. (1978).** Crystal structures of sodium sulfate decahydrate (Glauber's salt) and sodium tetraborate decahydrate (borax). Redetermination by neutron diffraction. *Structural Science*, 34(12), 3502-3510.
21. **Pudritz, R. E., Ouyed, R., Fendt, C., & Brandenburg, A. (2007).** Disk winds, jets, and outflows: Theoretical and computational foundations. *Protostars and Planets V*, 277–294.
22. **Rao, R., Girart, J. M., Lai, S. P., & Marrone, D. P. (2013).** Detection of a magnetized disk around a very young protostar. *The Astrophysical Journal Letters*, 780(1), L6.
23. **Salmeron, R., & Ireland, T. R. (2012).** Formation of chondrules in magnetic winds blowing through the proto-asteroid belt. *Earth and Planetary Science Letters*, 327, 61-67.
24. **Shakura, N. I., & Sunyaev, R. A. (1973).** Black holes in binary systems: Observational appearance. *Astronomy & Astrophysics*, 24, 337–355.
25. **Suriano, S. S., Li, Z.-Y., Krasnopolsky, R., & Shang, H. (2018).** Global non-ideal MHD simulations of the inner regions of protoplanetary disks. *The Astrophysical Journal*, 869(2), 115.
26. **Testi, L., Birnstiel, T., Ricci, L., Andrews, S., Blum, J., Carpenter, J., ... & Wilner, D. J. (2014).** Dust evolution in protoplanetary disks. *Protostars and planets VI*, 339.
27. **Turner, N. J., Fromang, S., Gammie, C., Klahr, H., Lesur, G., Wardle, M., & Bai, X.-N. (2014).** Transport and accretion in planet-forming disks. *Protostars and Planets VI*, 411–432.
28. **Wardle, M. (2007).** Magnetic fields in protoplanetary disks. *Astrophysics and Space Science*, 311(1), 35–45.
29. **Wardle, M., & Salmeron, R. (2012).** Hall effect and the magnetorotational instability in protoplanetary disks. *Monthly Notices of the Royal Astronomical Society*, 422(4), 2737–2747.
30. **Williams, J. P., & Cieza, L. A. (2011).** Protoplanetary disks and their evolution. *Annual Review of Astronomy and Astrophysics*, 49(1), 67-117.
31. **Woitke, P., Min, M., Pinte, C., Thi, W. F., Kamp, I., Rab, C., ... & Spaans, M. (2016).** Consistent dust and gas models for protoplanetary disks-I. Disk shape, dust settling, opacities, and PAHs. *Astronomy & Astrophysics*, 586, A103.
32. **Wurster, J., Bate, M. R., & Price, D. J. (2016).** Can non-ideal magnetohydrodynamics solve the magnetic braking catastrophe? *Monthly Notices of the Royal Astronomical Society*, 457, 1037–1061.
33. **Yang, H., Li, Z. Y., Looney, L., & Stephens, I. (2016).** Inclination-induced polarization of scattered millimetre radiation from protoplanetary discs: the case of HL Tau. *Monthly Notices of the Royal Astronomical Society*, 456(3), 2794-2805.